



# Development of an effective fluorescence probe for discovery of aminopeptidase inhibitors to suppress biofilm formation

Tianhu Zhao<sup>1</sup> · Jian Zhang<sup>1</sup> · Maomao Tang<sup>2,3</sup> · Luyan Z. Ma<sup>2,3</sup> · Xiaoguang Lei<sup>1</sup> 

Received: 10 December 2018 / Revised: 28 January 2019 / Accepted: 28 February 2019 / Published online: 20 March 2019  
© The Author(s), under exclusive licence to the Japan Antibiotics Research Association 2019

## Abstract

The human pathogen *Pseudomonas aeruginosa* can easily form biofilms. The extracellular matrix produced by the bacterial cells acts as a physical barrier to hinder the antibiotics treatment. It is necessary to destroy the biofilm in order to improve the efficacy of antibiotics. However, it has been a significant challenge to develop effective small molecules targeting the components of biofilm matrix. In this study, we report the development of a new effective fluorescence probe that could be used in the high throughput screening to identify novel small molecule inhibitors targeting the most abundant component in the biofilm formation: *P. aeruginosa* aminopeptidase (PaAP). Through screening of an in-house chemical library, a commercially available drug, balsalazide, has been identified as a novel PaAP inhibitor, which exhibited remarkable anti-biofilm effect. Our study indicated that the newly developed fluorescence probe is applicable in exploring new aminopeptidase inhibitors, and it also warrants further investigation of balsalazide as a new anti-biofilm agent to treat *P. aeruginosa* infection in combination with known antibiotics.

## Introduction

*Pseudomonas aeruginosa* is a ubiquitous environmental microorganism, and is also a major human pathogen causing life-threatening infections in immuno-compromised patients [1–4]. *P. aeruginosa* infections are difficult to

treat, not only due to its intrinsic resistance to many antibiotics [5], but also because of its ability to form biofilms wherein the bacterial cells are encased in an extracellular polymeric substance (EPS) matrix [6–8]. The biofilm matrix can serve as a protective barrier for bacteria to escape the antimicrobial therapies and host immune responses, thus leading to significant morbidity and mortality [9–11]. Nowadays, *P. aeruginosa* is one of the top three “critical priority pathogens” on the WHO priority list.

To eradicate *P. aeruginosa* biofilm infections, scientists have tried to destroy the EPS matrix, which consists of mainly polysaccharides, proteins, and extracellular DNA (eDNA) [12], to improve the antibiotic access to the EPS-enmeshed bacterial cells [13–17]. *P. aeruginosa* aminopeptidase (PaAP) is one of the most abundant matrix proteins in *P. aeruginosa* biofilms [18]. Previous studies have shown that PaAP contributes to maintain *P. aeruginosa* biofilm biomass in the late stage of biofilm formation by recycling nutrients within biofilms, and the loss of PaAP results in substantial cell death and biofilm disruption (Fig. 1) [19], suggesting PaAP as a potential therapeutic target for the treatment of *P. aeruginosa* infection.

Aminopeptidase is a major type of exopeptidase that releases amino acids from the N-terminus of the peptide or protein substrates [20]. PaAP belongs to leucine aminopeptidase, which preferentially catalyzes the hydrolysis of

**Supplementary information** The online version of this article (<https://doi.org/10.1038/s41429-019-0166-z>) contains supplementary material, which is available to authorized users.

✉ Luyan Z. Ma  
luyanma27@im.ac.cn

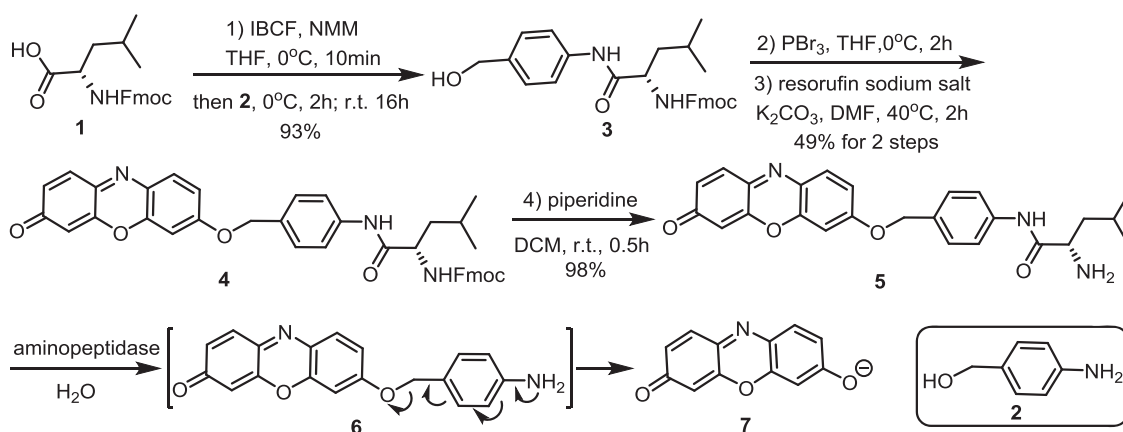
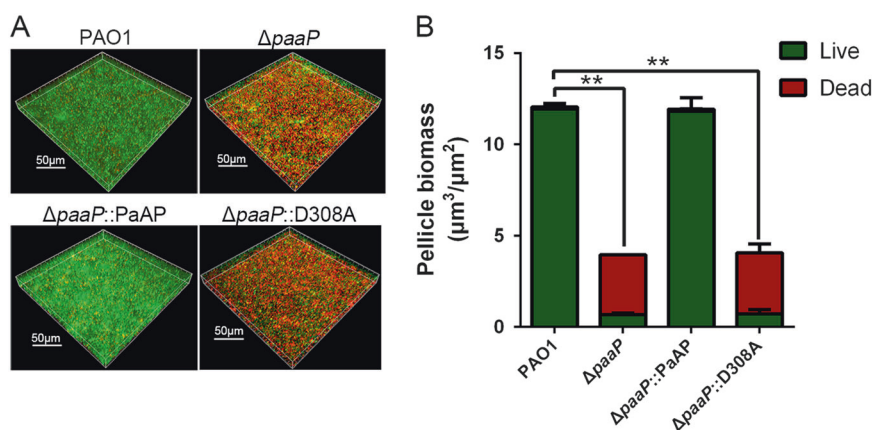
✉ Xiaoguang Lei  
xglei@pku.edu.cn

<sup>1</sup> Department of Chemical Biology, College of Chemistry and Molecular Engineering, Beijing National Laboratory for Molecular Sciences, Key Laboratory of Bioorganic Chemistry and Molecular Engineering of Ministry of Education, Synthetic and Functional Biomolecules Center and Peking-Tsinghua Center for Life Sciences, Peking University, 100871 Beijing, China

<sup>2</sup> State Key Laboratory of Microbial Resources, Institute of Microbiology, Chinese Academy of Sciences, 100101 Beijing, China

<sup>3</sup> University of Chinese Academy of Sciences, 100049 Beijing, China

**Fig. 1** Loss of PaAP resulted in bacterial cell death and biofilm disruption [19]. **a** Live/dead staining of the biofilms of *P. aeruginosa* wild type PAO1, *paaP* in frame deletion strain  $\Delta paaP$ , *paaP* recover strain  $\Delta paaP::PaAP$ , and  $\Delta paaP$  with point-mutated *paaP* gene  $\Delta paaP::D308A$  after 48 h of growth. The three-dimensional reconstituted images pellicles were shown. Live bacteria were stained green with SYTO9. Dead bacteria were stained red with propidium iodide. **b** The corresponding quantification of live and dead biomass of the pellicles was shown in panel **a**



**Scheme 1** Synthesis of probe 5 and the enzymatic reaction with aminopeptidase

leucine residues at the N-terminus of peptides and proteins [21]. Traditionally, *L*-Leu-*p*-nitroanilide is used as the substrate to evaluate the aminopeptidase activity by detecting the increased absorbance at 405 nm due to the release of *p*-nitroaniline [21–23]. However, such reaction is not very sensitive because of the demands for high concentrations of protein and substrate. Besides, the reaction is carried out at 50–60 °C [22], which is not the optimal temperature (37 °C) for *P. aeruginosa* growth, suggesting that the potential PaAP inhibitors identified using *L*-Leu-*p*-nitroanilide might not be effective at 37 °C. To search for the potential new PaAP inhibitors through high throughput screening (HTS), a more sensitive probe is required.

Resorufin-based fluorescence “off–on” chemical probe has been widely studied for the detection of enzyme activity [24, 25]. Here we adopted this general strategy to design and prepare a type of spectroscopic “off–on” chemical probe (5; Scheme 1) by linking *L*-leucine with resorufin-based fluorescence “off–on” probe to detect the activity of *P. aeruginosa* aminopeptidase. Resorufin was chosen as a fluorescence unit owing to its good water solubility, long analytical wavelength

(λ<sub>570/585</sub> nm), and efficient fluorescence quenching via alkylation of the 7-hydroxy group [26]. We further developed a robust HTS assay with this new fluorescence “off–on” probe, and subsequently using this assay identified nine PaAP small molecule inhibitors via HTS. One of them, named balsalazide (Fig. 2, compound 8), exhibited remarkable inhibition effect against the biofilm formation. Our data suggested that this newly developed fluorescence probe is applicable in exploring aminopeptidase inhibitors, and it also warrants further investigation of balsalazide as a new anti-biofilm agent to treat *P. aeruginosa* infection in combination with known antibiotics.

## Result

### The synthesis of fluorescence probe for detecting aminopeptidase activity

The synthesis was commenced with the condensation between Fmoc-*L*-leucine 1 and *p*-aminobenzyl alcohol 2.

Bromination of **3** followed by Williamson ether synthesis to afford intermediate **4**. Deprotection of Fmoc protecting group of **4** afforded probe **5** (Scheme 1). **5** shows minimal fluorescence due to the quenching action of the phenylmethoxy unit, which is favorable due to the low background signal. Treatment of **5** with aminopeptidase in the presence of H<sub>2</sub>O resulted in the hydrolysis of the amide bond, followed by the cascade 1,6-elimination of intermediate **6** to release resorufin **7** and turn on the fluorescence signal (Scheme 1).

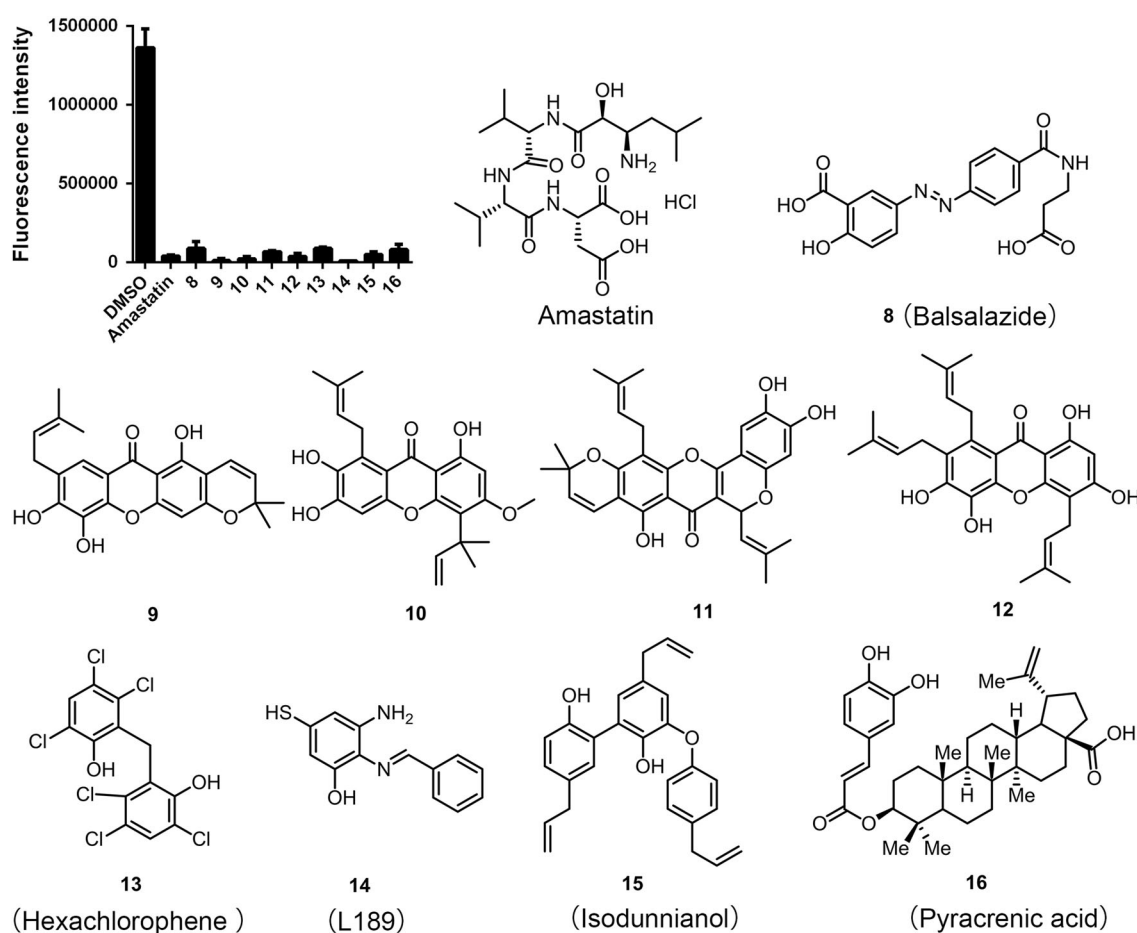
### The fluorescence probe **5** is more effective than the traditional probe

To search for the potential PaAP inhibitors through HTS effectively, a robust assay is required where the signal change before/after the enzymatic reaction should be significant enough (normally greater than 10-fold). Thus, the sensitivity of the newly developed fluorescence probe **5** and the traditional substrate *L*-Leu-*p*-nitroanilide was compared

by the signal change of fluorescence intensity or OD<sub>405</sub>, respectively, before/after the enzymatic reactions (Table 1 and Table 2). Six hundred micromolar of *L*-Leu-*p*-nitroanilide was first used according to the reported protocol [21], and its sensitivity was detected using different concentrations of PaAP protein. As shown in Table 1, the biggest change of OD<sub>405</sub> before/after reaction was 7.4 fold when using 50 µg/mL PaAP, which was not significant enough. The sensitivity of fluorescence probe **5** was evaluated using different concentrations of probe and different concentrations of PaAP protein. The reaction was carried out at

**Table 1** Sensitivity of the traditional substrate

PaAP (µg/mL)	OD <sub>405</sub> fold change
100	6.18 ± 0.11
50	7.42 ± 0.09
20	2.28 ± 0.23
10	0.10 ± 0.01

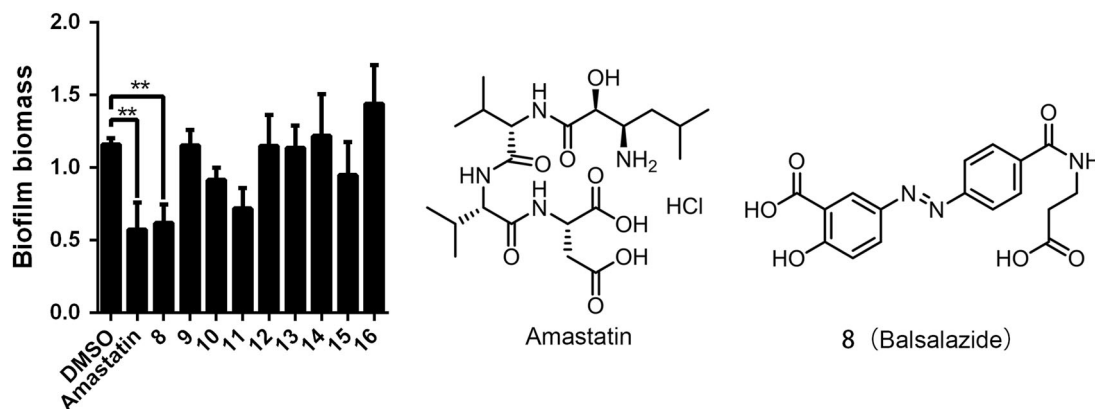
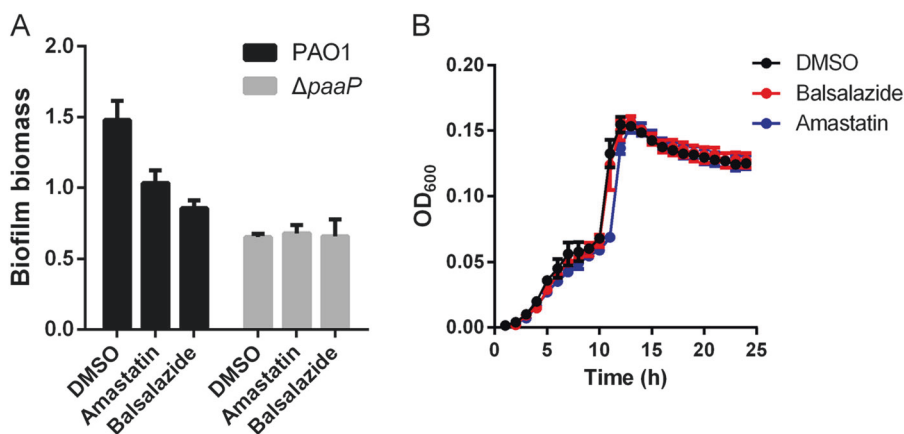


**Fig. 2** The potential PaAP inhibitors identified from HTS. The inhibition effect of the PaAP potential inhibitors on the PaAP enzymatic activity detected using the fluorescence probe **5** was shown in the columns, and the chemical structures were shown. Amastatin was used as the positive control

**Table 2** Sensitivity of fluorescence probe 5

PaAP ( $\mu\text{g/mL}$ )	Probe concentration ( $\mu\text{M}$ )				
	5	2.5	1.25	0.5	0.25
15	13.27 $\pm$ 0.12	<b>31.28 <math>\pm</math> 0.10</b>	18.10 $\pm$ 0.18	11.79 $\pm$ 0.21	12.63 $\pm$ 0.73
10	10.18 $\pm$ 0.09	22.83 $\pm$ 0.31	10.90 $\pm$ 0.17	9.92 $\pm$ 0.30	8.71 $\pm$ 0.14
5	11.39 $\pm$ 0.25	9.92 $\pm$ 0.22	4.00 $\pm$ 0.31	3.62 $\pm$ 0.14	5.60 $\pm$ 0.35

Bold value: The biggest change of fluorescence intensity before/after reaction in the experiment

**Fig. 3** The anti-biofilm effect of the identified PaAP potential inhibitors. Balsalazide was identified as the most promising inhibitor**Fig. 4** The inhibition effect of balsalazide on biofilm formation was mainly due to the inhibition of PaAP activity. **a** The effect of balsalazide on the biofilm formation of *P. aeruginosa* wild type PAO1 and *paaP* in frame deletion strain  $\Delta paaP$ . **b** The growth curves of *P. aeruginosa* PAO1 treated with 10  $\mu\text{M}$  of balsalazide, amastatin, or DMSO

37 °C, the optimal growth temperature for *P. aeruginosa*. The biggest change of fluorescence intensity before/after reaction was 31.3-fold when using 15  $\mu\text{g/mL}$  PaAP and 2.5  $\mu\text{M}$  fluorescence probe 5 (Table 2). Comparing with the traditional substrate  $L$ -Leu-*p*-nitroanilide, we could detect PaAP activity with less amount of PaAP protein using this new fluorescence probe 5, and the fluorescence intensity change before/after reaction was four-fold higher than OD<sub>405</sub> signal change, suggesting that fluorescence probe 5 was more sensitive than the traditional substrate  $L$ -Leu-*p*-nitroanilide in detecting the PaAP activity.

### HTS using probe 5 reveals potential new PaAP inhibitors

A library of ~7000 small molecules in-house were screened for the potential PaAP inhibitors using the newly established system (15  $\mu\text{g/mL}$  PaAP and 2.5  $\mu\text{M}$  fluorescence probe 5). The naturally occurring, competitive, and reversible aminopeptidase inhibitor amastatin was used as the positive control substrate. Through this endeavor, we identified nine PaAP inhibitors (Fig. 2) exhibiting better or

comparable activity than amastatin. Balsalazide **8** is an FDA approved drug for the treatment of mild to moderate ulcerative colitis [27]. Compounds **9–12** share structural similarities and belong to prenylated xanthone natural product [28, 29]. Hexachlorophene **13** has been used as a disinfectant [30, 31]. L189 **14** is a novel human DNA ligase inhibitor [32]. Compound **15** is also a triphenyl-neolignan type of natural product named isodunnianol [33]. Pyracrenic acid **16** is a triterpenoid [34].

### The validation of anti-biofilm effect of the potential PaAP inhibitors

To validate the anti-biofilm effect of PaAP inhibitors, 10  $\mu\text{M}$  of each compound was added at inoculation. As shown in Fig. 3, compared to the positive control amastatin, compound **8** (balsalazide) showed the most potent anti-biofilm effect among all the newly identified PaAP inhibitors. The anti-biofilm effect of balsalazide was further detected between wild-type *P. aeruginosa* PAO1 and *paaP* in frame deletion strain  $\Delta paaP$ , which does not express PaAP, to determine whether balsalazide selectively targeted PaAP to inhibit the *P. aeruginosa* biofilm formation. Balsalazide had no effect on the biofilm formation of  $\Delta paaP$  (Fig. 4a). Notably, bacterial growth was not affected by the addition of balsalazide at the concentration tested (Fig. 4b), suggesting that balsalazide inhibited *P. aeruginosa* biofilm formation not because of the inhibition of bacterial growth, but due to the inhibition of aminopeptidase activity.

### Discussion

*Pseudomonas aeruginosa* is one of the most significant pathogens that cause clinical problems due to its ability to form biofilms [6–8]. The highly heterogeneous extracellular polymeric substance biofilm matrix secreted by the bacterial cells makes the standard antibiotic treatments unsuccessful [35–37]. *P. aeruginosa* aminopeptidase (PaAP), as one of the most abundant matrix proteins and an important component in *P. aeruginosa* biofilms, has become a potential therapeutic target for preventing *P. aeruginosa* infections [18, 19]. Therefore, seeking PaAP inhibitors might help us to inhibit *P. aeruginosa* biofilm formation.

In this paper, in order to identify the potential new PaAP inhibitors, we have developed a fluorescence probe by linking L-leucine with resorufin-based fluorescence “off-on” probe to detect the enzymatic activity of PaAP. This new assay has shown better sensitivity than the traditional aminopeptidase substrate L-Leu-*p*-nitroanilide. This fluorescence probe **5** enables us to use less amount of PaAP protein and probe in the high throughput screening with higher sensitivity. Using this synthetic fluorescence probe,

nine PaAP potential inhibitors were identified by HTS. Among them, an FDA approved drug, balsalazide (compound **8**), exhibited remarkable inhibition effect on the biofilm formation of wild-type *P. aeruginosa* PAO1, but had no influence on the biofilm formation of *paaP* in frame deletion strain  $\Delta paaP$ . As a commercial available drug, the safety of balsalazide on human has already been tested. Further study is required to evaluate whether balsalazide is effective for treating *P. aeruginosa* infections in combination with known antibiotics.

### Materials and methods

#### General

$^1\text{H}$  NMR spectra were recorded on a Bruker 400 MHz spectrometer at ambient temperature with  $\text{CDCl}_3$  as the solvent unless otherwise stated.  $^{13}\text{C}$  NMR spectra were recorded on a Bruker 101 MHz, 126 MHz, or 151 MHz spectrometer (with complete proton decoupling) at ambient temperature. Chemical shifts are reported in parts per million relative to chloroform ( $^1\text{H}$ ,  $\delta$  7.26 ppm;  $^{13}\text{C}$ ,  $\delta$  77.00 ppm) or dimethyl sulfoxide ( $^1\text{H}$ ,  $\delta$  2.53 ppm;  $^{13}\text{C}$ ,  $\delta$  39.53 ppm). Data for  $^1\text{H}$  NMR are reported as follow: chemical shift, integration, multiplicity (*s* = singlet, *d* = doublet, *t* = triplet, *q* = quartet, *m* = multiplet), and coupling constants. High-resolution mass spectra were obtained at Peking University Mass Spectrometry Laboratory using a Bruker Fourier Transform Ion Cyclotron Resonance Mass Spectrometer Solarix XR. The samples were analyzed by HPLC/MS on a Waters Auto Purification LC/MS system (3100 Mass Detector, 2545 Binary Gradient Module, 2767 Sample Manager, and 2998 Photodiode Array (PDA) Detector). The system was equipped with a Waters C18 5  $\mu\text{m}$  SunFire separation column (150 $\times$ 4.6 mm), equilibrated with HPLC grade water (solvent A), and HPLC grade methanol (solvent B) with a flow rate of 0.3 mL/min at rt. Analytical thin layer chromatography was performed using 0.25 mm silica gel 60-F plates. Flash chromatography was performed using 200–400 mesh silica gel. Yields refer to chromatographically and spectroscopically pure materials, unless otherwise stated. All reagents were used as supplied by Sigma-Aldrich, J&K, and Alfa Aesar Chemicals. All reactions were carried out in oven-dried glassware under an argon atmosphere unless otherwise noted.

(9*H*-fluoren-9-yl)methyl (*S*)-(1-((4-(hydroxymethyl)phenyl)amino)-4-methyl-1-oxopentan-2-yl)carbamate (**2**)

Fmoc-Leu-OH (0.18 g, 0.50 mmol) was dissolved in 5 mL of tetrahydrofuran under argon flow and the solution was cooled to  $-10^\circ\text{C}$  in a 1:3 NaCl: ice bath. *N*-methylmorpholine (NMM, 0.11 mL, 1.0 mmol) and isobutyl chloroformate (0.065 mL, 0.50 mmol) were added dropwise with stirring. After 15 min, *p*-aminobenzyl alcohol (0.10 g,



0.50 mmol) was added and the reaction was allowed to proceed with stirring under argon flow at  $-10^{\circ}\text{C}$  for 2 h. The reaction was then allowed to proceed overnight with stirring at room temperature under an argon atmosphere for 20 h in total. The crude reaction mixture was concentrated in vacuo and diluted with 8 mL of ethyl acetate (EtOAc). This organic solution was extracted with 1 M  $\text{Na}_2\text{HPO}_4$ , brine, 5%  $\text{NaHCO}_3$ , and brine, 8 mL of each, subsequently. The combined aqueous solution was extracted with 10 mL of EtOAc. The combined organic mixture was then evaporated and run on a flash column in  $\text{DCM}/\text{MOH} = 100:1$ . The purified product was evaporated to dryness to afford white solid **4** (213 mg, 0.465 mmol, 93% yield).  $^1\text{H}$  NMR (400 MHz,  $\text{CDCl}_3$ )  $\delta$  8.14–7.93 (br, 1 H), 7.76 (d,  $J = 7.5$  Hz, 2 H), 7.56 (d,  $J = 7.2$  Hz, 2 H), 7.47 (d,  $J = 8.0$  Hz, 2 H), 7.39 (t,  $J = 7.4$  Hz, 2 H), 7.32–7.26 (m, 4 H), 5.25–5.11 (m, 1 H), 4.64 (s, 2 H), 4.51–4.40 (m, 2 H), 4.34–4.24 (m, 1 H), 4.21 (t,  $J = 6.5$  Hz, 1 H), 1.84–1.74 (m, 1 H), 1.73–1.63 (m, 2 H), 1.0–0.89 (m, 6 H).  $^{13}\text{C}$  NMR (101 MHz,  $\text{CDCl}_3$ )  $\delta$  170.6, 143.6, 141.3, 136.9, 127.7, 127.1, 124.9, 120.0, 67.2, 64.8, 54.2, 47.0, 40.9, 24.7, 22.9. ESI<sup>+</sup>-MS:  $[\text{M} + \text{H}]^+$  calculated for  $\text{C}_{28}\text{H}_{31}\text{N}_2\text{O}_4^+$ : 459.2278; found: 459.2281.

(9*H*-fluoren-9-yl)methyl (*S*)-(4-methyl-1-oxo-1-((4-(((3-oxo-3*H*-phenoxazin-7-yl)oxy)methyl)phenyl)amino)pentan-2-yl)carbamate (**4**)

Phosphorus tribromide (52.3  $\mu\text{L}$ , 0.556 mmol) was added to an ice-cooled solution of **3** (170 mg, 0.371 mmol) in THF (6 mL). The mixture was stirred at  $0^{\circ}\text{C}$  for 2 h before it was neutralized with ice-cold saturated aqueous  $\text{NaHCO}_3$  solution (2 mL) and further diluted with water (20 mL). The resulting solution was extracted with EtOAc ( $3 \times 10$  mL). The combined extracts were dried over  $\text{MgSO}_4$  and the solvent was removed under reduced pressure. The crude product was directly used in next step without further purification. To a suspension of resorufin sodium salt (87.2 mg, 0.371 mmol) in anhydrous DMF (5 mL) was added  $\text{K}_2\text{CO}_3$  (102 mg, 0.742 mmol), followed by stirring at  $40^{\circ}\text{C}$  for 10 min under argon atmosphere. A solution of crude product in DMF (5 mL) was added dropwise. The resulting mixture was stirred at  $40^{\circ}\text{C}$  for 2 h and then diluted with dichloromethane (50 mL). The organic layer was separated, washed with water ( $50$  mL  $\times 3$ ), and brine ( $50$  mL  $\times 3$ ), and then dried over  $\text{Na}_2\text{SO}_4$ . The solvent was removed under reduced pressure, and the residue was further purified by flash column in  $\text{CH}_2\text{Cl}_2/\text{MeOH} = 100:1$  to afford **4** as an orange solid (119 mg, 0.182 mmol 49%).  $^1\text{H}$  NMR (400 MHz, DMSO)  $\delta$  10.13 (s, 1 H), 7.89 (d,  $J = 7.5$  Hz, 2 H), 7.77 (d,  $J = 8.9$  Hz, 1 H), 7.73 (dd,  $J = 7.3, 4.5$  Hz, 2 H), 7.69 (d,  $J = 8.1$  Hz, 1 H), 7.65 (d,  $J = 8.5$  Hz, 2 H), 7.53 (d,  $J = 9.8$  Hz, 1 H), 7.47–7.38 (m, 4 H), 7.35–7.28 (m, 2 H), 7.19 (d,  $J = 2.5$  Hz, 1 H), 7.11 (dd,  $J = 8.9, 2.6$  Hz, 1 H), 6.78 (dd,  $J = 9.8, 2.0$  Hz, 1 H), 6.27 (d,  $J = 2.0$  Hz, 1 H), 5.22 (s, 2 H), 4.32–4.14 (m, 4 H), 1.75–1.55 (m, 2 H),

1.51–1.40 (m, 1 H), 0.99–0.88 (m, 6 H).  $^{13}\text{C}$  NMR (126 MHz, DMSO)  $\delta$  185.3, 171.6, 162.3, 156.0, 149.7, 145.20, 145.17, 143.9, 143.7, 140.7, 139.0, 134.9, 133.7, 131.3, 130.7, 128.7, 127.9, 127.6, 127.0, 125.3, 120.0, 119.3, 114.4, 105.6, 101.2, 70.1, 65.6, 53.8, 46.7, 24.3, 23.0, 21.5. ESI<sup>+</sup>-MS:  $[\text{M} + \text{H}]^+$  calculated for  $\text{C}_{40}\text{H}_{36}\text{N}_3\text{O}_6^+$ : 654.2599; found: 654.2603.

(*S*)-2-amino-4-methyl-*N*-(4-(((3-oxo-3*H*-phenoxazin-7-yl)oxy)methyl)phenyl) pentanamide (**5**)

Amide **4** (60 mg, 0.091 mmol) was dissolved in 20% piperidine in DMF (2 mL) and stirred at room temperature for 30 min. Solvent was removed and dissolved in  $\text{CH}_2\text{Cl}_2$  (10 mL) and  $\text{H}_2\text{O}$  (10 mL). The organic layer was separated and the aqueous layer was extracted with  $\text{CH}_2\text{Cl}_2$  (50 mL  $\times 3$ ). The combined organic extracts was dried over  $\text{Na}_2\text{SO}_4$ , then the solvent was removed under reduced pressure and the residue was further purified by a flash column in  $\text{CH}_2\text{Cl}_2/\text{MeOH} = 100:1$  to afford **5** as an orange solid (38 mg, 0.089 mmol 98%).  $^1\text{H}$  NMR (400 MHz,  $\text{CDCl}_3$ )  $\delta$  9.63 (s, 1 H), 7.80–7.55 (m, 3 H), 7.45–7.34 (m Hz, 3 H), 7.00 (d,  $J = 8.8$  Hz, 1 H), 6.88–6.80 (m, 2 H), 6.32 (s, 1 H), 5.14 (s, 2 H), 3.53 (d,  $J = 11.0$  Hz, 1 H), 1.86–1.74 (m, 1 H), 1.59–1.55 (m, 2 H), 0.99 (dd,  $J = 10.4, 5.8$  Hz, 6 H).  $^{13}\text{C}$  NMR (151 MHz,  $\text{CDCl}_3$ )  $\delta$  186.3, 173.8, 162.6, 157.7, 145.7, 145.6, 138.2, 134.7, 134.2, 131.6, 130.7, 128.4, 119.5, 114.3, 106.8, 101.1, 70.6, 53.9, 43.8, 25.0, 23.4, 21.3. ESI<sup>+</sup>-MS:  $[\text{M} + \text{H}]^+$  calculated for  $\text{C}_{25}\text{H}_{26}\text{N}_3\text{O}_4^+$ : 432.1918; found: 432.1919.

## Bacterial growth conditions

Unless indicated, *P. aeruginosa* strains were grown at  $37^{\circ}\text{C}$  in LB without sodium chloride (LBNS), and *E. coli* strains were grown at  $37^{\circ}\text{C}$  in Luria broth (LB). M9 medium (1 L: 2.54 g  $\text{Na}_2\text{HPO}_4$ , 1.5 g  $\text{KH}_2\text{PO}_4$ , 0.25 g  $\text{NaCl}$ , 0.5 g  $\text{NH}_4\text{Cl}$ , 11.11 mM glucose, 2 mM  $\text{MgSO}_4$ , and 0.1 mM  $\text{CaCl}_2$ ) was used to detect the effect of identified PaAP inhibitors on the growth of *P. aeruginosa* wild-type PAO1. The  $\text{OD}_{600}$  was measured every 1 hour using the Infinite F200 PRO Reader.

## The expression and purification of *P. aeruginosa* aminopeptidase

The plasmid used for PaAP expression was constructed according to Sarnovsky's method [23]. The primers PaAP-F (5'-AATCCCACATATGAAACCCAACCCGTCGA TC-3') and PaAP-R (5'-CGCAAGCTTGATGAAGTCGTGACCC-CAGC-3') were used to amplify the *paaP* gene (118bp-1605bp) from *P. aeruginosa* PAO1 genome by PCR. The resulting PCR product was digested with NdeI and Hind III, and cloned into plasmid pET29a to generate the recombinant plasmid rLAP53.

For PaAP expression, single colony of *E. coli* BL21 (DE3) carrying rLAP53 was growing in LB supplemented with kanamycin at 25 µg/mL overnight. Cells were 100 fold diluted from overnight cultures in fresh LB with kanamycin and grown at 37 °C to OD<sub>600</sub> ~0.5. The protein expression was induced with 0.1 mM isopropyl 1-thio-β-D-galactopyranoside at 16 °C for 16 h. Cells were harvested by centrifugation and resuspended in PBS buffer. Cells were broken by sonication, and the cell pellets (inclusion bodies) were resuspended in the washing buffer (0.5% Triton-100, 50 mM Tris, pH 8.0, 300 mM NaCl, 10 mM EDTA). The inclusion bodies were sonicated, centrifuged, and resuspended in the washing buffer for three times. The washed inclusion bodies were resuspended in the resuspending buffer (50 mM Tris, pH 8.0, 100 mM NaCl, 10 mM EDTA) at last time, sonicated again, and resuspended in dissolution buffer (6 M Guan-HCl, 10% glycerol, 50 mM Tris, pH 8.0, 100 mM NaCl). Denatured PaAP protein was refolded by adding guanidine-solubilized protein to the following solution: 0.5 M L-Arg, 50 mM Tris, pH 8.0, 1 mM CaCl<sub>2</sub>, 50 µM ZnCl<sub>2</sub>, pH 8.0, to a final protein concentration of ~50 µg/mL. Refolding was for 48 h at 10 °C. After refolding, PaAP protein was dialyzed against 20 mM Tris, pH 8.0, 50 mM NaCl, 1 mM CaCl<sub>2</sub>, 50 µM ZnCl<sub>2</sub>. The dialyzed PaAP solution was condensed, loaded onto a nickel affinity column (Chelating Sepharose Fast Flow, GE Healthcare), and washed with 30 mM imidazole for several times to remove the nonspecific proteins. The protein bound to the resin of nickel column was resuspended in 300 mM imidazole. The purified PaAP solution was condensed by ultrafiltration, and the solution buffer was changed to the buffer: 20 mM Tris, pH 8.0, 50 mM NaCl, 1 mM CaCl<sub>2</sub>, 50 µM ZnCl<sub>2</sub>.

### Aminopeptidase assay

The PaAP catalytic activity detected using the traditional substrate L-Leu-p-nitroanilide was determined according to previous research [21]. 0.6 mM L-Leu-p-nitroanilide was added at final concentration to 10, 20, 50, 100 µg/mL PaAP. The reaction was carried out at 50 °C for 15 min, and the OD<sub>405</sub> was measured before and after. The sensitivity of L-Leu-p-nitroanilide was evaluated by the fold change of OD<sub>405</sub>.

5 µM, 2.5 µM, 1.25 µM, 0.5 µM, and 0.25 µM fluorescence probe **5** was added at final concentration to 15, 10, 5 µg/mL PaAP, respectively. The reaction was carried out at 37 °C for 15 min, and the fluorescence intensity at 550 nm ex/580 nm em was measured before and after. The sensitivity of fluorescence probe **5** was evaluated by the fold change of fluorescence intensity.

### High throughput screening for PaAP inhibitors

The reaction was carried out using 2.5 µM fluorescence probe **5** and 15 µg/mL PaAP protein. The commercially available aminopeptidase inhibitor amastatin (CAS 100938-10-1) was used as the positive control. The tested compounds are stored at the Center For Life Sciences in Peking University. Ten micromolar of the tested compounds and amastatin were added to the reaction system at final concentration, and incubated at 37 °C for 15 min. The fluorescence intensity at 550 nm ex/580 nm em was measured before and after. The potential PaAP inhibitors were chosen, which could significantly inhibited the fluorescence intensity at 550 nm ex/580 nm em after reaction.

### Microtiter dish biofilm assay

The M9 medium was used to detect the screened aminopeptidase inhibitors on the *P. aeruginosa* biofilm formation. A 1/100 dilution of a saturated (overnight) *P. aeruginosa* culture in M9 medium was used for inoculation. The microtiter dishes were incubated at 30 °C for 12 h, and then the medium and planktonic cells were discarded. The biofilm was washed by PBS, stained with 0.1% crystal violet, and solubilized in 30% acetic acid, the OD<sub>560</sub> was measured to evaluate the biofilm biomass.

**Acknowledgements** This paper is dedicated to Prof. Samuel J. Danishefsky for his remarkable scientific career. Financial support from NNSFC (21625201, 21661140001, and 21521003), the National Key Research and Development Program of China (2017YFA0505200), and a research grant from Roche is acknowledged.

**Conflict of Interest** The authors declare that they have no conflict of interest.

**Publisher's note:** Springer Nature remains neutral with regard to jurisdictional claims in published maps and institutional affiliations.

### References

1. Gale MJ, Maritato MS, Chen Y-L, Abdulateef SS, Ruiz JE. *Pseudomonas aeruginosa* causing inflammatory mass of the nasopharynx in an immunocompromised HIV infected patient: a mimic of malignancy. *IDCases*. 2015;2:40–3.
2. Langan KM, Kotsimbos T, Peleg AY. Managing *Pseudomonas aeruginosa* respiratory infections in cystic fibrosis. *Curr Opin Infect Dis*. 2015;28:547–56.
3. Lund-Palau H, et al. *Pseudomonas aeruginosa* infection in cystic fibrosis: pathophysiological mechanisms and therapeutic approaches. *Expert Rev Respir Med*. 2016;10:685–97.
4. Lyczak JB, Cannon CL, Pier GB. Establishment of *Pseudomonas aeruginosa* infection: lessons from a versatile opportunist. *Microbes Infect*. 2000;2:1051–60.
5. Poole K. *Pseudomonas aeruginosa*: resistance to the max. *Front Microbiol*. 2011;2:65.

6. Costerton JW, Stewart PS, Greenberg EP. Bacterial biofilms: a common cause of persistent infections. *Science*. 1999;284:1318–22.
7. Drenkard E, Ausubel FM. *Pseudomonas* biofilm formation and antibiotic resistance are linked to phenotypic variation. *Nature*. 2002;416:740–3.
8. Stewart PS. Mechanisms of antibiotic resistance in bacterial biofilms. *Int J Med Microbiol*. 2002;292:107–13.
9. Ryder C, Byrd M, Wozniak DJ. Role of polysaccharides in *Pseudomonas aeruginosa* biofilm development. *Curr Opin Microbiol*. 2007;10:644–8.
10. Parsek MR, Singh PK. Bacterial biofilms: an emerging link to disease pathogenesis. *Annu Rev Microbiol*. 2003;57:677–701.
11. Haussler S, Parsek MR. Biofilms 2009: new perspectives at the heart of surface-associated microbial communities. *J Bacteriol*. 2010;192:2941–9.
12. Flemming HC, Wingender J. The biofilm matrix. *Nat Rev Microbiol*. 2010;8:623–33.
13. Brown A, et al. Blow fly *Lucilia sericata* nuclease digests DNA associated with wound slough/eschar and with *Pseudomonas aeruginosa* biofilm. *Med Vet Entomol*. 2012;26:432–9.
14. Yu S, et al. PslG, a self-produced glycosyl hydrolase, triggers biofilm disassembly by disrupting exopolysaccharide matrix. *Cell Res*. 2015;25:1352–67.
15. Banar M, et al. Evaluation of mannosidase and trypsin enzymes effects on biofilm production of *Pseudomonas aeruginosa* isolated from burn wound infections. *PLoS ONE*. 2016;11:e0164622.
16. Diaz De Rienzo MA, Stevenson PS, Marchant R, Banat IM. *Pseudomonas aeruginosa* biofilm disruption using microbial surfactants. *J Appl Microbiol*. 2016;120:868–76.
17. Ray VA, Hill PJ, Stover CK. Anti-Psl targeting of *Pseudomonas aeruginosa* biofilms for neutrophil-mediated disruption. *Sci Rep*. 2017;7:16065.
18. Toyofuku M, Roschitzki B, Riedel K, Eberl L. Identification of proteins associated with the *Pseudomonas aeruginosa* biofilm extracellular matrix. *J Proteome Res*. 2012;11:4906–15.
19. Zhao T, et al. Extracellular aminopeptidase modulates biofilm development of *Pseudomonas aeruginosa* by affecting matrix exopolysaccharide and bacterial cell death. *Environ Microbiol Rep*. 2018;10:583–93.
20. Gonzales T, Robert-Baudouy J. Bacterial aminopeptidases: properties and functions. *FEMS Microbiol Rev*. 1996;18:319–44.
21. Cahan R, Axelrad I, Safrin M, Ohman DE, Kessler E. A secreted aminopeptidase of *Pseudomonas aeruginosa*. Identification, primary structure, and relationship to other aminopeptidases. *J Biol Chem*. 2001;276:43645–52.
22. Gaur R, Grover T, Sharma R, Kapoor S, Khare SK. Purification and characterization of a solvent stable aminopeptidase from *Pseudomonas aeruginosa*: cloning and analysis of aminopeptidase gene conferring solvent stability. *Process Biochem*. 2010;45:757–64.
23. Sarnovsky R, et al. Proteolytic cleavage of a C-terminal prosequence, leading to autoprocessing at the N Terminus, activates leucine aminopeptidase from *Pseudomonas aeruginosa*. *J Biol Chem*. 2009;284:10243–53.
24. Li Z, Li X, Gao X, Zhang Y, Shi W, Ma H. Nitroreductase detection and hypoxic tumor cell imaging by a designed sensitive and selective fluorescent probe, 7-[(5-nitrofuranyl)methoxy]-3H-phenoxazin-3-one. *Anal Chem*. 2013;85:3926–32.
25. Wu X, Li X, Li H, Shi W, Ma H. A highly sensitive and selective fluorescence off-on probe for the detection of intracellular endogenous tyrosinase activity. *Chem Commun*. 2017;53:2443–6.
26. Zhou J, Ma H. Design principles of spectroscopic probes for biological applications. *Chem Sci*. 2016;7:6309–15.
27. Prakash A, Spencer CM. Balsalazide. *Drugs*. 1998;56:83–9. discussion 90
28. Chanmahasathien W, et al. Prenylated xanthenes from *Garcinia xanthochymus*. *Chem Pharm Bull*. 2003;51:1332–4.
29. Li Y, et al. Depsidone and xanthenes from *Garcinia xanthochymus* with hypoglycemic activity and the mechanism of promoting glucose uptake in L6 myotubes. *Bioorg Med Chem*. 2017;25:6605–13.
30. Einola S. Studies on the disinfectant properties of G-11 (hexachlorophene). *Ann Med Exp Biol Fenn*. 1955;33:1–54.
31. Kimbrough RD. Review of the toxicity of hexachlorophene. *Arch Environ Health*. 1971;23:119–22.
32. Howes TRL, et al. Structure-activity relationships among DNA ligase inhibitors: characterization of a selective uncompetitive DNA ligase I inhibitor. *DNA Repair (Amst)*. 2017;60:29–39.
33. Kouno I, Morisaki T, Hara Y, Yang C-S. Two new sesquiterpene lignans from the bark of *Illicium dunnianum*. *Chem Pharm Bull*. 1991;39:2606–8.
34. Chen B, Duan H, Takaishi Y. Triterpene caffeoyl esters and diterpenes from *Celastrus stephanotifolius*. *Phytochemistry*. 1999;51:683–7.
35. Belfield K, Bayston R, Hajduk N, Levell G, Birchall JP, Daniel M. Evaluation of combinations of putative anti-biofilm agents and antibiotics to eradicate biofilms of *Staphylococcus aureus* and *Pseudomonas aeruginosa*. *J Antimicrob Chemother*. 2017;72:2531–8.
36. Rybtke M, Hultqvist LD, Givskov M, Tolker-Nielsen T. *Pseudomonas aeruginosa* biofilm infections: community structure, antimicrobial tolerance and immune response. *J Mol Biol*. 2015;427:3628–45.
37. Taylor PK, Yeung AT, Hancock RE. Antibiotic resistance in *Pseudomonas aeruginosa* biofilms: towards the development of novel anti-biofilm therapies. *J Biotechnol*. 2014;191:121–30.